Mathematical Biosciences and Engineering

MBE, 17 (5): 4852–4874.
DOI: 10.3934/mbe.2020264
Received: 13 May 2020
Accepted: 08 July 2020
Published: 13 July 2020

http://www.aimspress.com/journal/MBE

Research article

Dual solutions in biomagnetic fluid flow and heat transfer over a nonlinear stretching/shrinking sheet: Application of lie group transformation method

Mohammad Ferdows [1,*], Ghulam Murtaza [1,2], Jagadis C. Misra [3], Efstratios E. Tzirtzilakis [4] and Abdulaziz Alsenafi [5]

[1] Research group of Fluid Flow Modeling and Simulation, Department of Applied Mathematics, University of Dhaka, Dhaka-1000, Bangladesh
[2] Department of Mathematics, Comilla University, Comilla-3506, Bangladesh
[3] Central for Healthcare Science and Technology, Indian Institute of Engineering Science and Technology, Shibpur, Howrah-711103, India
[4] Department of Mechanical Engineering, University of the Peloponnese, Patras, Greece
[5] Department of Mathematics, kuwait University P.O. Box 5969, Safat 13060, Kuwait

*** Correspondence:** Email: ferdows@du.ac.bd; Tell: +8801720809796.

Abstract: Of concern in the paper is a theoretical investigation of boundary layer flow of a biomagnetic fluid and heat transfer on a stretching/shrinking sheet in the presence of a magnetic dipole. The problem has been treated mathematically by using Lie group transformation. The governing nonlinear partial differential equations are thereby reduced to a system of coupled nonlinear ordinary differential equations subject to associated boundary conditions. The resulting equations subject to boundary conditions are solved numerically by using bvp4c function available in MATLAB software. The plots for variations of velocity, temperature, skin friction and heat transfer rate have been drawn and adequate discussion has been made. The study reveals that the problem considered admits of dual solutions in particular ranges of values of the suction parameter and nonlinear stretching/shrinking parameter. A stability analysis has also been carried out and presented in the paper. This enables one to determine which solution is stable that can be realized physically, and which is not. The results of the present study have been compared with those reported by previous investigators to ascertain the validity/reliability of the computational results.

Keywords: dual solutions; stability analysis; biomagnetic fluid; magnetic dipole

Nomenclature

(x, y): Cartesian coordinates; (u, v): velocity components in the x and y direction; (ξ, η): dimensionless coordinates; H: magnetic field intensity; Pr: Prandtl number; B: magnetic induction; B_0 ,saturation magnetic induction; M: fluid magnetization; M_s: saturation magnetization; T: fluid temperature; T_c: fluid temperature far away from sheet; T_w: temperature of the sheet; θ: dimensionless temperature; ρ: density of fluid; μ: dynamic viscosity; ν: kinematic viscosity; μ_0: magnetic permeability; c_p: specific heat constant pressure; k: thermal conductivity; λ_a: viscous dissipation parameter; ε: dimensionless temperature parameter; M_n: magnetohydrodynamic parameter; β: ferromagnetic interaction parameter; α, dimensionless distance; m: temperature exponent parameter; λ: stretching parameter.

1. Introduction

Studies on biomagnetic fluid flow and heat transfer under the influence of external magnetic fields have been receiving growing attention of researchers owing to their important applications in bioengineering and clinical sciences. Observations derived from related investigation are useful in the design and development of magnetic devices for cell separation, reduction of blood flow during surgery, targeted transport of drugs through the use of magnetic particles as drug carriers, magnetic resonance imaging (MRI) of specific parts of the human body, electromagnetic hyperthermia in cancer treatment etc., as mentioned in earlier communications (see [1–3]).

Base on the principles of Ferrohydrodynamics (FHD), a biomagnetic fluid model was developed [4]. This was further extended [5] by combining the principles of Magnetohydrodynamics with those of FHD and applied his model to analyze the flow of blood under the influence of a magnetic field. In [6] the authors studied the flow of a heated ferrofluid over a linearly stretching sheet under the action of a magnetic field generated due to the presence of a magnetic dipole. Laminar two-dimensional flow of an incompressible biofluid over a stretching sheet was studied numerically [7]. The effect of heat transfer on the flow behaviour was also studied by these authors. Flows of biomagnetic viscoelastic fluids in different situations were investigated theoretically [2,3]. These studies reveal that the presence of external magnetic field bears the potential of influencing the flow behaviour of biomagnetic viscoelastic fluids quite appreciably. The mathematical analysed of biomagnetic fluid with stretching sheet [8]. Their model developed by the principles of ferrohydrodynamic and magnetohydrodynamic. In [9] authors presented the biomagnetic fluid over a stretching cylinder. Their problem is formulated by a BFD model which incorporates both principles of FerroHydroDynamics (FHD) and MagnetoHydroDynamics (MHD). In [10] authors discussed the mathematical modelling of the ferro-nanofluid flow with nanoparticles and microorganisms. In [11] authors discussed the theoretical study on the swimming of migratory gyrotactic microorganisms in a non-Newtonian blood flow based nanofluid via an anisotropically narrowing artery. In [12] authors

also analyzed the heat transfer properties and the applications of the blood clot model with variable viscosity. In [13] authors also reported the peristaltic blood flow of Sisko fluid with magnetic nanoparticle and they considered Titanium magneto-nanoparticles.

Existence of dual solutions has been reported in various studies by different researchers. Some of them have presented stability analysis also. Mukhopadhyay [14] while dealing with a problem of heat transfer in a moving fluid over a moving flat surface observed the existence of dual solutions. Vajravelu et al. [15] while studying the unsteady flow and heat transfer over a shrinking sheet, with consideration of thermal radiation and viscous dissipation reported the existence of dual solutions for the flow field. In [16] authors observed dual solutions for an unsteady problem of flow past an inclined sheet. In [17] authors found the existence of dual solutions during MHD stagnation point flow over a stretching/shrinking sheet. It was reported [18] that dual solutions exist for boundary layer flow and heat transfer over an exponentially stretching/shrinking sheet. In [19] also discussed the existence of dual solutions for MHD stagnation point flow over a shrinking surface with partial slip. The multiple solutions of magnetohydrodynamic fluid flow and heat transfer of non-Newtonian fluid past a permeable nonlinear shrinking sheet involving convective boundary condition were studied by [20]. Stability analysis has presented in several studies (see [21–23]).

Use of Lie group transformation method has been found to be very effective in finding the solutions of highly nonlinear differential equations. It helps determine the invariants and similarity solutions for partial differential equations (see [24,25]). Several researchers (see [26–30]) have used Lie group analysis method for dealing with various problems of fluid flow and heat transfer.

Several problems of flow and heat transfer on sheets/channels under the action of external magnetic/electric fields that have applications to physiological fluid dynamics have been treated mathematically among others by Misra and his collaborators [31-36]. The flow and heat transfer of MHD blood as a third-grade non-Newtonian fluid conveying gold nanoparticles in the porous area of hollow vessel analyzed [37]. They considered the viscosity of nanofluid is considered a function of temperature. The numerical solutions of the MHD flow through a porous medium over a stretching sheet were studied [38]. The flow of a power law liquid by a stretchable surface subject to Joule heating, convective boundary conditions, Activation energy and viscous dissipation effects is examined [39]. In [40] authors analyzed the magnetohydrodynamic and thermal radiation on the unsteady flow of a Newtonian liquid through stagnation point due to a linear sheet with mass transpiration. The mixed convection heat transfer combined with thermal radiation of a viscoelastic liquid circulation driven by a porous accelerating sheet under the inclined uniform magnetic field impact were studied by [41].

However, in none of these studies, stability analysis/existence of multiple solutions has been considered. More particularly, to the best of our knowledge, there has not been any attempt to explore the existence of multiple solutions or to discuss the stability for any theoretical analysis for the flows of biomagnetic fluids. With this end in view an attempt has been made in this paper to explore the stability and existence of dual solutions in the context of flow and heat transfer of biomagnetic fluids on stretching/shrinking sheets. The governing equations being highly nonlinear, we have made use of the Lie group transformation method. Finally, the computational results have been obtained with the help of bvp4c function available in Matlab software. Detailed discussion has been made for variations of biomagnetic fluid velocity, temperature, skin friction and heat transfer rate. The study reveals that there exist dual solutions in specific ranges of the vital parameters involved and that one of the two solutions is stable and physically realistic. The validity of the

numerical results presented has also been established.

2. Proposed methodology: Problem formulation, working principle and modeling

2.1. Problem formulation

Let us consider the two-dimensional incompressible boundary layer flow and heat transfer of a biomagnetic fluid over a stretching/shrinking sheet (Figure 1), where $\bar{x}-$axis is taken along the sheet and $\bar{y}-$axis along the normal direction. We assume that stretching/shrinking has a velocity $\bar{u}=a\bar{x}^{n}$, where $a(>0)$ is a constant that signifies the stretching situation. When $a<0,$ we have the case of a shrinking sheet. It is assumed that the free stream velocity is $U_{\infty}(x)=b\bar{x}^{n}$, where b is a positive constant. A magnetic dipole is supposed to be located below the sheet at a distance d which generates a magnetic field of constant strength. Also, we denote the temperature of the sheet by $T_w(\bar{x})$ and the ambient temperature by $T_c(\bar{x})$.

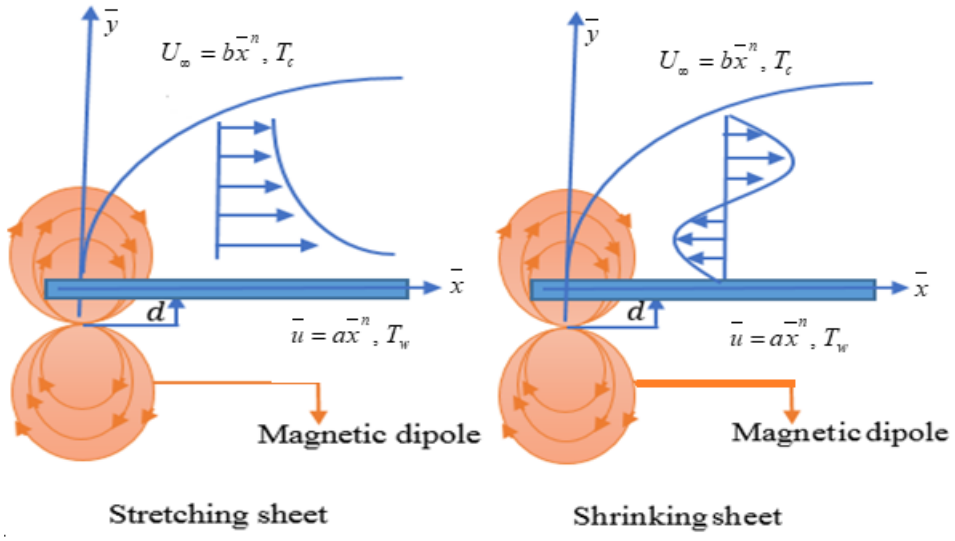

Figure 1. The geometry of the problem.

Under the assumptions of boundary layer approximation, as well as assumptions for the magnetic field i.e. it is strong enough to attain saturation magnetization and the induced magnetic field is negligible, the governing equations for the problem considering both electrical conductivity and polarization can be written as [5, 8]

$$\frac{\partial \bar{u}}{\partial \bar{x}}+\frac{\partial \bar{v}}{\partial \bar{y}}=0 \tag{1}$$

$$\bar{u}\frac{\partial \bar{u}}{\partial \bar{x}}+\bar{v}\frac{\partial \bar{u}}{\partial \bar{y}}=\bar{U}_{\infty}\frac{\partial \bar{U}_{\infty}}{\partial \bar{x}}+\bar{\nu}\frac{\partial^2 \bar{u}}{\partial \bar{y}^2}+\frac{\mu_0}{\rho}M\frac{\partial H}{\partial \bar{x}}+\frac{\sigma B^2(\bar{x})}{\rho}\left(\bar{U}_{\infty}-\bar{u}\right) \tag{2}$$

$$\rho c_p\left(\bar{u}\frac{\partial T}{\partial \bar{x}}+\bar{v}\frac{\partial T}{\partial \bar{y}}\right)+\mu_0 T\frac{\partial M}{\partial T}\left(\bar{u}\frac{\partial H}{\partial \bar{x}}+\bar{v}\frac{\partial H}{\partial \bar{y}}\right)=k\frac{\partial^2 T}{\partial \bar{y}^2} \tag{3}$$

and the boundary conditions as

$$\bar{u}=u_w(x)=a\bar{x}^n,\ v=v_w(\bar{x}),\ T=T_w=\left(T_{\infty}-D\bar{x}^m\right)\ \ at\ \bar{y}=0$$

$$\bar{u}=U_{\infty}(x)=b\bar{x}^n,\ T\to T_c\quad as\ \bar{y}\to\infty. \tag{4}$$

$\bar{u}$ and $\bar{v}$ being the velocity components along the $\bar{x}-$ and $\bar{y}-$ axes, respectively. Other parameters ρ and k represent respectively the fluid density and the thermal conductivity. c_p is the specific heat at constant pressure, μ the fluid viscosity and μ_0 the magnetic permeability. We consider that the magnetic field strength varies linearly with temperature T, M as a linear function of temperature T, given by $M=K(T_c-T)$, K being a constant.

The horizontal and vertical components of the magnetic field generated by a magnetic dipole located at a distance d below the sheet are given by (cf. [7])

$$H_x(x,y)=-\frac{\gamma}{2\pi}\frac{y+d}{x^2+(y+d)^2}\quad \text{and}\quad H_y(x,y)=\frac{\gamma}{2\pi}\frac{x}{x^2+(y+d)^2}$$

Then, the magnitude $\|H\|=H$ of the magnetic field is given by

$$H(x,y)=\left[H_x^2+H_y^2\right]^{1/2}=\frac{\gamma}{2\pi}\frac{1}{\sqrt{x^2+(y+d)^2}}\approx\frac{\gamma}{2\pi}\left[\frac{1}{(y+d)^2}-\frac{1}{2}\frac{x^2}{(y+d)^4}\right] \tag{5}$$

2.2. Mathematical analysis

We now introduce the following dimensionless quantities:

$$x=\frac{b}{c}\bar{x},\ y=\sqrt{\frac{(n+1)b}{2\nu}}\bar{y},\ u=\frac{\bar{u}}{c},\ v=\sqrt{\frac{(n+1)}{2\nu b}}\bar{v},\ U_{\infty}=\frac{\bar{U}_{\infty}}{c},\ \theta(\eta)=\frac{T_c-T}{T_c-T_w} \tag{6}$$

where c is a characteristic velocity.
Substituting (6) into Equations (1)-(3), one obtains the non-dimensional equations:

$$u\frac{\partial u}{\partial x}+v\frac{\partial u}{\partial y}=U_\infty\frac{\partial U_\infty}{\partial x}+\frac{n+1}{2}\frac{\partial^2 u}{\partial y^2}-\frac{(n+1)^2}{4}\frac{2\beta\theta x}{(y+d)^4}+M_n.x^{n-1}(U_\infty-u) \tag{7}$$

$$\left(u\frac{\partial\theta}{\partial x}+v\frac{\partial\theta}{\partial y}\right)+\frac{k\mu_0}{\rho c_p}(\varepsilon-\theta)\left(u\frac{\partial H}{\partial x}+v\frac{\partial H}{\partial y}\right)=\frac{1}{\Pr}\frac{n+1}{2}\frac{\partial^2\theta}{\partial y^2} \tag{8}$$

in which $\beta=\frac{\gamma}{2\pi}\frac{\mu_0 k(T_c-T_w)\rho}{\mu^2}$, $\Pr=\frac{\mu c_p}{k}$, $M_n=\frac{\sigma B_0^2}{\rho a}$, $\varepsilon=\frac{T_c}{(T_c-T_w)}$.

Further, on introducing a stream function ψ, where $u=\frac{\partial\psi}{\partial y}, v=-\frac{\partial\psi}{\partial x}$, the eqs (7) and (8) assume the form

$$\frac{\partial\psi}{\partial y}\frac{\partial^2\psi}{\partial x\partial y}-\frac{\partial\psi}{\partial x}\frac{\partial^2\psi}{\partial^2 y}=U_\infty\frac{\partial U_\infty}{\partial x}+\frac{n+1}{2}\frac{\partial^3\psi}{\partial y^3}+M_n x^{n-1}\left(U_\infty-\frac{\partial\psi}{\partial y}\right)-\frac{(n+1)^2}{4}\frac{2\beta\theta x}{(y+d)^4} \tag{9}$$

$$\frac{\partial\psi}{\partial y}\frac{\partial\theta}{\partial x}-\frac{\partial\psi}{\partial x}\frac{\partial\theta}{\partial x}+\frac{k\mu_0}{\rho c_p}(\varepsilon-\theta)\left(\frac{\partial\psi}{\partial y}\frac{\partial H}{\partial x}-\frac{\partial\psi}{\partial x}\frac{\partial H}{\partial y}\right)=\frac{1}{\Pr}\frac{n+1}{2}\frac{\partial^2\theta}{\partial y^2} \tag{10}$$

where the dimensionless form of the boundary conditions expressed in terms of ψ are obtained as

$$\frac{\partial\psi}{\partial y}=ax^n,\ \frac{\partial\psi}{\partial x}=-\frac{v_w}{\sqrt{\frac{2\nu b}{n+1}}},\ \theta=1 \quad at\ \ y=0$$

and $\frac{\partial\psi}{\partial y}=U_\infty=bx^n,\ \theta=0 \quad as\ \ y\to\infty$. (11)

2.3. Lie group transformation

Since it is extremely difficult to solve the coupled nonlinear equations (9) and (10) subject to the boundary conditions (11) even numerically, we resort to the application of a novel type of similarity transformation, called the Lie group transformation (alternatively called the scaling group transformation) given by [30]

$$\begin{aligned}&\Gamma: x^*=xe^{\varepsilon\alpha_1},\ y^*=ye^{\varepsilon\alpha_2},\ \psi^*=\psi e^{\varepsilon\alpha_3},\ u^*=ue^{\varepsilon\alpha_4},\ v^*=ve^{\varepsilon\alpha_5},\ U_\infty{}^*=U_\infty e^{\varepsilon\alpha_6},\\ &\theta^*=\theta e^{\varepsilon\alpha_7},\ H^*=He^{\varepsilon\alpha_8}\end{aligned} \tag{12}$$

Here ε is the group scaling parameter and α_i $(i=1,2,...,8)$ are arbitrary real numbers. Now we find

out the values of α_i such that the form of (9)-(11) is invariant under the scaling group transformation (12). This transformation can be treated as point transformation, which transforms the coordinates $(x, y, \psi, u, v, U_\infty, \theta, H)$ to $(x^*, y^*, \psi^*, u^*, v^*, U_\infty^*, \theta^*, H^*)$

Substituting (12) into (9) and (10), we get

$$e^{\varepsilon(\alpha_1+2\alpha_2-2\alpha_3)}\left(\frac{\partial\psi^*}{\partial y^*}\frac{\partial^2\psi^*}{\partial x^*\partial y^*}-\frac{\partial\psi^*}{\partial x^*}\frac{\partial^2\psi^*}{\partial y^{*2}}\right)=e^{\varepsilon(\alpha_1-2\alpha_6)}U_\infty^*\frac{\partial U_\infty^*}{\partial x^*}+\frac{n+1}{2}e^{\varepsilon(3\alpha_2-\alpha_3)}\frac{\partial^3\psi^*}{\partial y^{*3}}$$

$$+Mx^{*n-1}e^{\varepsilon(\alpha_1-n\alpha_1-\alpha_6)}U_\infty^*+Mx^{*n-1}e^{\varepsilon(\alpha_1-n\alpha_1+\alpha_2-\alpha_3)}\frac{\partial\psi^*}{\partial y^*}-\frac{(n+1)^2}{4}\frac{2\beta\theta^*x^*}{(y^*+d)^4}e^{\varepsilon(4\alpha_2-\alpha_1-\alpha_7)} \tag{13}$$

and $e^{\varepsilon(\alpha_1+\alpha_2-\alpha_3-\alpha_7)}\left(\frac{\partial\psi^*}{\partial y^*}\frac{\partial\theta^*}{\partial x^*}-\frac{\partial\psi^*}{\partial x^*}\frac{\partial\theta^*}{\partial y^*}\right)+\frac{k\mu_0}{\rho c_p}e^{\varepsilon(\alpha_1+\alpha_2-\alpha_3-\alpha_8)}\left(\frac{\partial\psi^*}{\partial y^*}\frac{\partial H^*}{\partial x^*}-\frac{\partial\psi^*}{\partial x^*}\frac{\partial H^*}{\partial y^*}\right)$

$$-\frac{k\mu_0}{\rho c_p}\theta^*e^{\varepsilon(\alpha_1+\alpha_2-\alpha_3-\alpha_7-\alpha_8)}\left(\frac{\partial\psi^*}{\partial y^*}\frac{\partial H^*}{\partial x^*}-\frac{\partial\psi^*}{\partial x^*}\frac{\partial H^*}{\partial y^*}\right)=\frac{1}{\mathrm{Pr}}\frac{n+1}{2}\frac{\partial^2\theta^*}{\partial y^{*2}}e^{\varepsilon(2\alpha_2-\alpha_7)} \tag{14}$$

The transformed equations (13) and (14) are invariant under the Lie group of transformation, if the following relations among the transform parameters are satisfied.

$$\alpha_1+2\alpha_2-2\alpha_3=\alpha_1-2\alpha_6=3\alpha_2-\alpha_3=\alpha_1-n\alpha_1-\alpha_6=\alpha_1-n\alpha_1+\alpha_2-\alpha_3=4\alpha_2-\alpha_1-\alpha_7 \tag{15}$$

and $$\alpha_1+\alpha_2-\alpha_3-\alpha_7=\alpha_1+\alpha_2-\alpha_3-\alpha_8=\alpha_1+\alpha_2-\alpha_3-\alpha_7-\alpha_8=2\alpha_2-\alpha_7 \tag{16}$$

By using the equations (15)-(16) and the boundary conditions we obtain

$$\alpha_2=-\frac{n+1}{2}\alpha_1,\alpha_3=\frac{n+1}{2}\alpha_1,\ \alpha_6=n\alpha_1,\alpha_7=0,\ \alpha_8=0,\alpha_4=n\alpha_1,\alpha_5=\frac{n-1}{2}\alpha_1 \tag{17}$$

If we insert (17) into the scaling (12), the set of transformations reduces to a one parameter group of transformations given by

$\Gamma: x^*=xe^{\varepsilon\alpha_1},\ y^*=ye^{\varepsilon\frac{n-1}{2}\alpha_1},\ \psi^*=\psi e^{\varepsilon\frac{n+1}{2}\alpha_1},\ u^*=ue^{\varepsilon n\alpha_1},\ v^*=ve^{\varepsilon\frac{n-1}{2}\alpha_1},\ U_\infty^*=U_\infty e^{\varepsilon n\alpha_1},\ \theta^*=\theta$ and

$H^*=H.$

Expanding by Tailor's method and remaining terms up to $O(\varepsilon^2)$ of the one parameter group, we further get

$$x^*-x=x\varepsilon\alpha_1+o(\varepsilon^2),\ y^*-y=-y\varepsilon\frac{n-1}{2}\alpha_1+o(\varepsilon^2),\ \psi^*-\psi=\psi\varepsilon\frac{n+1}{2}\alpha_1+o(\varepsilon^2),$$

$$u^*-u=u\varepsilon n\alpha_1+o(\varepsilon^2),\ v^*-v=v\varepsilon\frac{n-1}{2}\alpha_1+o(\varepsilon^2),\ U_\infty^*-U_\infty=U_\infty\varepsilon n\alpha_1,\ \theta^*-\theta=0$$

and $H^* - H = 0.$ (18)

From Eq. (18), one can easily deduce the set of transformation in the form of the following characteristic equations:

$$\frac{dx}{x\alpha_1} = \frac{dy}{-\frac{n-1}{2}y\alpha_1} = \frac{d\psi}{\frac{n+1}{2}\psi\alpha_1} = \frac{du}{un\alpha_1} = \frac{dv}{\frac{n-1}{2}v\alpha_1} = \frac{dU_\infty}{nU_\infty\alpha_1} = \frac{d\theta}{0} = \frac{dH}{0} \tag{19}$$

Integrating the subsidiary equations

$$\frac{dx}{x\alpha_1} = \frac{dy}{-\frac{n-1}{2}y\alpha_1},$$

we get $yx^{\frac{n-1}{2}} = \eta$ (say)

From the subsidiary equations

$$\frac{dx}{x\alpha_1} = \frac{d\theta}{0},$$

we get $d\theta = 0,$ that is $\theta(\eta) =$ constant $= \theta$ (say).

Also integrating the equation $\frac{dx}{x\alpha_1} = \frac{d\psi}{\frac{n+1}{2}\psi\alpha_1},$

we get $\frac{\psi}{x^{\frac{n+1}{2}}} = = f(\eta)$ (say)

i.e. $\psi = x^{\frac{n+1}{2}} f(\eta)$

Thus the new similarity transformations are obtained as follows:

$$\eta = yx^{\frac{n-1}{2}}, \psi = x^{\frac{n+1}{2}} f(\eta), \theta = \theta(\eta) \tag{20}$$

Substitution of (20) into (9)-(11), yields the system of nonlinear ordinary differential equations given below

$$f''' + ff'' - \frac{2n}{n+1}(f'^2 - 1) + \frac{2M_n}{n+1}(1 - f') - \frac{n+1}{2}\frac{2\beta\theta}{(\eta+\alpha)^4} = 0 \tag{21}$$

and $$\theta'' - \Pr\left(\frac{2m}{n+1}f'\theta - f\theta'\right) + \frac{2\lambda_a\beta(\varepsilon-\theta)f}{(\eta+\alpha)^3} = 0 \tag{22}$$

The associated boundary conditions are:

$$\begin{aligned} &f = S,\ f' = \lambda,\ \theta = 1 \quad at \quad \eta = 0 \\ &f' \to 1,\ \theta \to 0 \qquad as \quad \eta \to \infty \end{aligned} \tag{23}$$

in which $\beta = \frac{\gamma}{2\pi}\frac{\mu_0 k(T_c - T_w)\rho}{\mu^2}$, $\lambda_a = \frac{\mu^2}{\rho k(T_c - T_w)}$, $\mathrm{Pr} = \frac{\mu c_p}{k}$, $M_n = \frac{\sigma B_0^2}{\rho a}$, $\varepsilon = \frac{T_c}{(T_c - T_w)}$, $\alpha = \sqrt{\frac{a\rho}{\mu}}$. Also $\lambda = \frac{a}{b}$ is the stretching/shrinking parameter, where $\lambda > 0$ indicates the stretching sheet, $\lambda < 0$ represents the shrinking sheet and $S = \frac{2v_w}{\sqrt{2(n+1)\nu b}\, x^{(n-1)/2}}$ is the suction/injection parameter where suction defined by $S > 0$ and $S < 0$ refers to injection.

The important physical characteristics skin friction coefficient C_{fx} and the local Nusselt number Nu_x are described as $C_{fx} = \frac{\tau_w}{\frac{1}{2}\rho u_w^2}$ and $Nu_x = \frac{xq_w}{k(T_c - T_w)}$ (24)

In Eqn. (24), τ_w is the shear stress at wall, while q_w represents the wall heat flux, defined by

$$\tau_w = \mu\left(\frac{\partial u}{\partial y}\right)_{y=0} \text{ and } q_w = -k\left(\frac{\partial T}{\partial y}\right)_{y=0} \tag{25}$$

Introducing (25) into Eqn. (24), the skin friction coefficient and local Nusselt number can be written in dimensionless form as

$$\frac{1}{2}C_{fx}\sqrt{\mathrm{Re}_x} = f''(0) \quad \text{and} \quad Nu_x / \sqrt{\mathrm{Re}_x} = -\theta'(0) \tag{26}$$

where $\mathrm{Re}_x = \frac{u_w(x)x}{\nu}$ is the local Reynolds number based on the stretching velocity $u_w(x)$.

2.4. Stability analysis

In this section, we present a stability analysis for the unsteady flow of the biomagnetic fluid, by considering the momentum equation in the form

$$\frac{\partial u}{\partial t} + u\frac{\partial u}{\partial x} + v\frac{\partial u}{\partial y} = U_\infty \frac{\partial U_\infty}{\partial x} + \frac{n+1}{2}\frac{\partial^2 u}{\partial y^2} - \frac{(n+1)^2}{4}\frac{2\beta\theta x}{(y+d)^4} + M_n . x^{n-1}(U_\infty - u) \tag{27}$$

$$\frac{\partial \theta}{\partial t}+\left(u\frac{\partial \theta}{\partial x}+v\frac{\partial \theta}{\partial y}\right)+\frac{k\mu_0}{\rho c_p}(\varepsilon-\theta)\left(u\frac{\partial H}{\partial x}+v\frac{\partial H}{\partial y}\right)=\frac{1}{\Pr}\frac{n+1}{2}\frac{\partial^2\theta}{\partial y^2} \tag{28}$$

where t denotes the time. Here we define another set of dimensionless variables (in tune with equation (20)) as

$$\psi = x^{\frac{n+1}{2}} f(\eta,\tau),\ \eta = yx^{\frac{n-1}{2}},\ \tau = tx^{n-1},\ \theta = \theta(\eta,\tau)$$

In terms of these variables, the expression for the axial and transverse velocities read

$$u = x^n \frac{\partial f}{\partial \eta}(\eta,\tau) \quad \text{and} \quad v = -x^{\frac{n-1}{2}}\frac{n+1}{2}\left[f(\eta,\tau)+\frac{n-1}{n+1}\eta\frac{\partial f}{\partial \eta}(\eta,\tau)-2\frac{n-1}{n+1}\tau\frac{\partial f}{\partial \eta}(\eta,\tau)\right] \tag{29}$$

Substituting (29) in equation (27) and (28), we have

$$\frac{\partial^3 f}{\partial \eta^3}+f\frac{\partial^2 f}{\partial \eta^2}-\frac{2n}{n+1}\left(\frac{\partial f}{\partial \eta}\right)^2+\frac{2n}{n+1}+\frac{2M_n}{n+1}\left(1-\frac{\partial f}{\partial \eta}\right)-\frac{n+1}{2}\frac{2\beta\theta}{(\eta+\alpha)^4}-\frac{2}{n+1}\frac{\partial^2 f}{\partial \eta\partial \tau}$$

$$-\frac{2(n-1)}{n+1}\tau\frac{\partial f}{\partial \tau}\frac{\partial^2 f}{\partial \eta^2}=0, \tag{30}$$

$$\frac{\partial^2\theta}{\partial \eta^2}-P_r\left(\frac{2m}{n+1}\frac{\partial f}{\partial \eta}\theta-f\frac{\partial \theta}{\partial \eta}+\frac{\partial \theta}{\partial \tau}-\tau\frac{\partial f}{\partial \eta}\frac{\partial \theta}{\partial \tau}+\tau\frac{\partial f}{\partial \tau}\frac{\partial \theta}{\partial \eta}\right)+\frac{2\lambda_a\beta(\varepsilon-\theta)f}{(\eta+\alpha)^3}=0 \tag{31}$$

The associated boundary conditions being

$$f(0,\tau)=S,\ \frac{\partial f}{\partial \eta}(0,\tau)=\lambda,\frac{\partial \theta}{\partial \eta}(0,\tau)=1$$

and $$\frac{\partial f}{\partial \eta}(\eta,\tau)\to 0,\theta(\eta,\tau)\to 0\ as\ \eta\to\infty \tag{32}$$

To test the stability of the steady flow solution $f(\eta)=F(\eta)$, $\theta(\eta)=\theta_0(\eta)$ that satisfy the boundary value problem (2) and (3), we write

$$f(\eta,\tau)=F(\eta)+e^{-\gamma\tau}g(\eta,\tau),$$

$$\theta(\eta,\tau)=\theta_0(\eta)+e^{-\gamma\tau}G(\eta,\tau) \tag{33}$$

where γ is an unknown eigenvalue parameter and $g(\eta,\tau)$ and $G(\eta,\tau)$ are small as compared to $F(\eta)$ and $\theta_0(\eta)$. By substituting (33) into equation (30) and (31), we get the following linearized

problem:

$$\frac{\partial^3 g}{\partial \eta^3}+F\frac{\partial^2 g}{\partial \eta^2}+g\frac{\partial^2 F}{\partial \eta^2}-\frac{2n}{n+1}2\frac{\partial g}{\partial \eta}\frac{\partial F}{\partial \eta}-\frac{2M_n}{n+1}\frac{\partial g}{\partial \eta}+\frac{2}{n+1}\gamma\frac{\partial g}{\partial \eta}-\frac{2}{n+1}\frac{\partial^2 g}{\partial \eta\partial \tau}-$$

$$\frac{2(n-1)}{n+1}\tau\left(\frac{\partial^2 g}{\partial \eta\partial \tau}-\gamma g\right)\frac{\partial^2 F}{\partial \eta^2}=0 \tag{34}$$

$$\frac{\partial^3 G}{\partial \eta^3}+\Pr\left(F\frac{\partial G}{\partial \eta}+\gamma G+g\frac{\partial \theta_0}{\partial \eta}-G\frac{\partial F}{\partial \eta}-2\theta_0\frac{\partial g}{\partial \eta}\right)-\frac{2\beta\lambda_a\varepsilon g}{(\eta+\alpha)^3}+\frac{2\beta\lambda_a(FG+\theta_0 g)}{(\eta+\alpha)^3}=0 \tag{35}$$

subject to the boundary conditions:

$$g(0,\tau)=0,\frac{\partial g}{\partial \eta}(0,\tau)=0,G(0,\tau)=0$$

and $\frac{\partial g}{\partial \eta}(\eta,\tau)\to 0, G(0,\tau)\to 0 \; as \;\; \eta\to\infty$ (36)

For $\tau=0,$ we have $f(\eta)=F(\eta) and\ \theta(\eta)=\theta_0(\eta)$ we have the case of steady flow of the fluid characterized by equation (21), while $g(\eta)=g_0(\eta)$ and $G(\eta)=G_0(\eta)$ in (34) and (35) characterizes the initial growth or decay of the solution (33). To test our numerical procedure, the following linear eigenvalue problem corresponding to the steady state problem:

$$g_0'''+Fg_0''+g_0F''-\frac{4n}{n+1}F'g_0'-\frac{2M_n}{n+1}g_0'+\frac{2}{n+1}\gamma g_0'=0 \tag{37}$$

$$G_0''+\Pr\left(FG_0'+g_0\theta_0'-g_0F'+\gamma G_0+g_0'\theta_0'\right)-\frac{2\beta\lambda\varepsilon g_0}{(\eta+\alpha)^3}+\frac{2\beta\lambda(FG_0+\theta_0 g_0)}{(\eta+\alpha)^3}=0 \tag{38}$$

along with the conditions:

$$g_0(0)=0,\;\; g_0'(0)=0,G_0(0)=0$$

and $g_0'(\eta)\to 0,\ G_0(0)\to 0 \quad as \quad \eta\to\infty.$ (39)

The smallest eigenvalue γ will determine the stability of the corresponding steady flow solution $F(\eta)$ for all the parameters involved. Hence the boundary condition of $g_0'(\eta)\to 0\ as\ \eta\to\infty$ can be relaxed as suggested by Harris et al. [45] and replace by a new

boundary condition $g_0''(0)=1.$

2.4. Numerical scheme

Now we solve the set of nonlinear ordinary differential equations (21) and (22) with boundary conditions (23) numerically by using bvp4c function technique in MATLAB package. We consider $f=y_1,\ f'=y_2,\ f''=y_3,\theta=y_4,\theta'=y_5$. Then the equations (7) and (8) are transformed into a system of first order ordinary differential equations as given below.

$$\left.\begin{aligned} f' &= y_2 \\ f'' &= y_2' = y_3 \\ f''' = y_3' &= -y_1y_3+\frac{2n}{n+1}(y_2^2-1)-\frac{2M_n}{n+1}(1-y_2)+\frac{n+1}{2}\frac{2\beta y_4}{(\eta+\alpha)^4} \\ \theta' &= y_5 \\ \theta'' = y_5' &= -\Pr y_1y_5+\frac{2m}{n+1}\Pr y_2y_4-\frac{2\lambda_a\beta(\varepsilon-y_4)y_1}{(\eta+\alpha)^3} \end{aligned}\right\} \tag{40}$$

along with the initial boundary conditions:

$$y_1(0)=S,\ y_2(0)=\lambda,\ y_4(0)=1,\ y_2(\infty)=1,\ y_4(\infty)=0. \tag{41}$$

Equations (40) and (41) are integrated numerically as an initial value problem to a given terminal point. All these simplifications are made by using bvp4c function available in MATLAB software.

3. Results and discussion

The nonlinear ordinary differential equations (21) and (22) with boundary conditions (23), can be solved numerically using the bvp4c programme in MATLAB software. In order to continue to the derivation of the numerical results it is necessary to allocate values to the dimensionless parameters. For this problem, assume that the fluid is blood with $\rho=1050\,kg/m^3$ and $\mu=3.2\times10^{-3}\,kgm^{-1}s^{-1}$ [1]. The electrical conductivity of blood is $\sigma=0.8sm^{-1}$ [5], and the temperature of the fluid is $T_c=41^0c$ whereas the plate temperature is $T_w=37^0c$. As it is known, for temperatures above 41°C, blood cell irreversible structural damages occur, and this is the reason why someone's life is in danger if he/she is exposed to such high fever. This biological limit of 41°C is by definition the Curie Temperature, T_c, of blood since the definition of T_c in general Ferrohydrodynamics is the temperature, beyond of which, we no longer have the magnetization effect on the fluid $(M_n=0)$ [5]. For the above values of temperature, the temperature number is $\varepsilon=78.5$ [8] and the viscous dissipation number is 6.4×10^{-14} [8]. Generally, the specific heat under a constant pressure c_p and thermal conductivity k

of any fluid are temperature dependent. However, the ratio including the above quantities expressed by the Prandtl number can be considered constant with the temperature variation. Therefore, for the temperature range consider in this problem, $c_p = 3.9\times10^3\ Jkg^{-1}k^{-1}$ and $k = 0.5\,Jm^{-1}s^{-1}k^{-1}$ and hence $P_r = 25$ [6,8]. As far as the parameters related with the magnetic field, in the present study we adopted the values of β to be from 0 to 10, used also in the study of [1, 6, 8].

In order to establish the validity and accuracy of the method, we have computed the skin friction coefficient for steady flow with $\beta = 0,\ S = 0, M_n = 0,\ n = 1$ and compared with previous studies, as shown in Table 1. The computations of $f''(0)$ in [42, 43] were done by using the bvp4c solver and shooting method, respectively. Thus, the usage of these studies in validating the method used in the present study was suitable. It was found that the results were in good agreement. This reassured that the method used was accurate.

Table 1. Comparison of skin friction coefficient ($f''(0)$) for different values of λ with $\beta = 0,\ S = 0, M_n = 0,\ n = 1$.

λ	Present		Naganthran et.al [42]		Bhattacharyya[43]	
	First solution	Second solution	First solution	Second solution	First solution	Second solution
-0.25	1.402239		1.402240		1.4022405	
-0.5	1.49567		1.495669		1.4956697	
-0.75	1.48929		1.489298		1.4892981	
-1.0	1.32882	0.00126	1.328816	0	1.3288169	0
-1.15	1.08225	0.11576	1.082231	0.116702	1.0822316	0.1167023
-1.2	0.93253	0.23286	0.932473	0.233649	0.9324728	0.2336491

While carrying out numerical computation, we observe that dual solutions exist for a certain range of stretching/shrinking of the sheet and suction parameter. Since the dual solutions exist, we need to ascertain which solution is physically meaningful. With this end in view, we have performed stability analysis. For the sake of brevity, the details of the stability analysis are not being presented here. However, on the basis of the stability test, we find that one set of solutions is stable and physically realizable, while the other solution set is not so.

Figures 2–7 depict the existence of dual solutions for skin friction $f''(0)$ and wall heat transfer gradient $\theta'(0)$ for different values of the stretching/shrinking parameter and the suction parameter, when the value of ferromagnetic parameter and nonlinear stretching parameter changes.

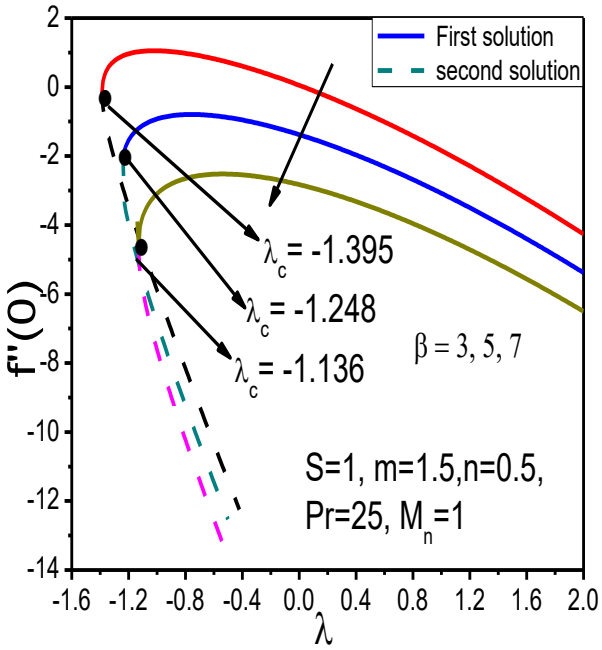

Figure 2. Variation of skin friction coefficient with λ for various values of β.

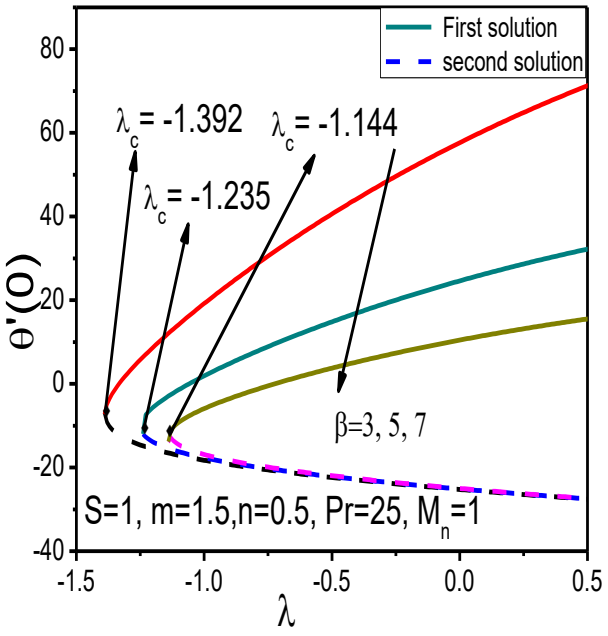

Figure 3. Variation of heat transfer rate with λ for different values of β.

The graphs presented in Figures 2 and 3 have been plotted by considering different values of the ferromagnetic parameter and so they clearly depict the ferromagnetic effect of the fluid. It is interesting to note that there exist two solution branches. The first branch represents the stable solution, while the second branch denotes the unstable solution for each value of λ corresponding to a given value of β. From Figure 2, we observe that unique solution exists for $\lambda > -0.2$ or $\lambda > -0.3$ or $\lambda > -0.4$ when $\beta = 3,5,7$ respectively, while dual solutions exist when $-1.395 < \lambda < -0.4$ for $\beta = 7$, when $-1.248 < \lambda < -0.3$ for $\beta = 5$ and when $-1.136 < \lambda < -0.2$ for $\beta = 3$. Also no solution exists when $\lambda < \lambda_c$, where $\lambda_c = -1.136, -1.248, -1.395$ for $\beta = 3,5,7.$ respectively, λ_c being the critical value of λ, at which the two solution branches meet each other and thus a unique solution is obtained.

Variation of wall heat transfer rate $\theta'(0)$ with stretching parameter for various values of the ferromagnetic parameter are shown in Figure 3. From this figure, it can be seen that the solution is unique when $\lambda = \lambda_c$, while dual solutions exist when $\lambda_c < \lambda < 0.5$ and no solutions exist, when $\lambda < \lambda_c$, where λ_c is the critical value of λ and the value of $\lambda_c = -1.392, -1.235, -1.144$ with specific values of $\beta = 3,5,7.$ From this figure we also observe that the critical value λ_c decreases, as the value of the ferromagnetic parameter increases and that of the skin friction coefficient

decreases. One way further observe that the effect of the ferromagnetic parameter diminishes in the range of λ for which the solution exists.

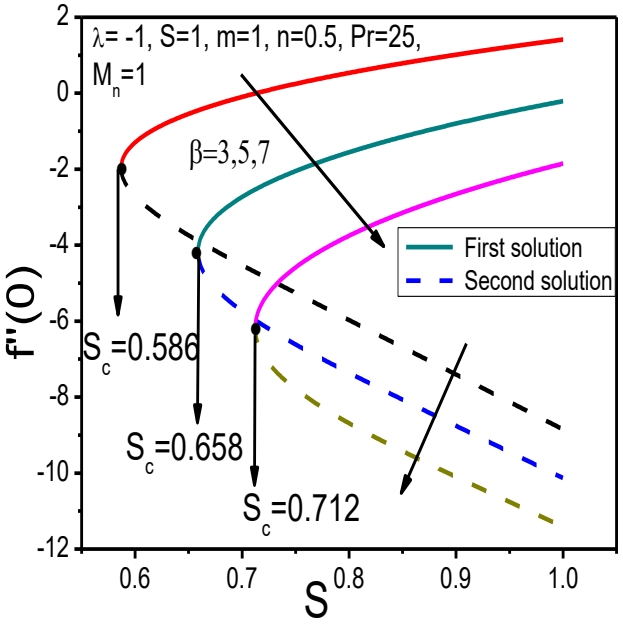

Figure 4. Variation of skin friction coefficient With S for various values of β.

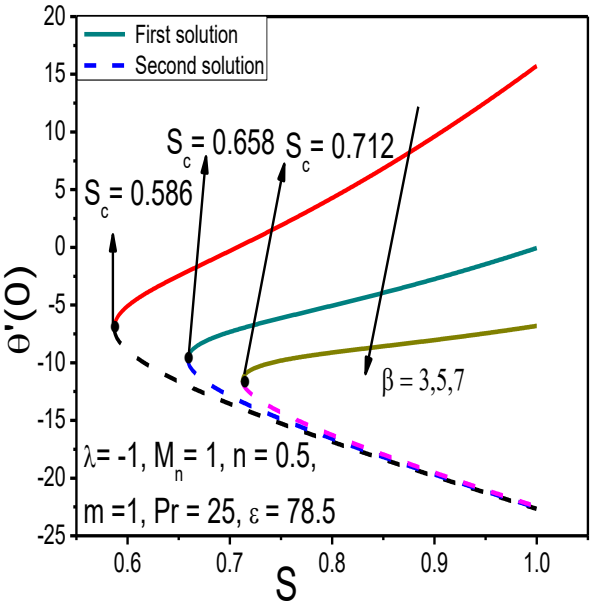

Figure 5. Variation of heat transfer rate with S for various values of β.

The variations of the skin friction coefficient $f''(0)$ and the local Nusselt number $\theta'(0)$ with suction parameter for different values of the ferromagnetic parameter are shown in figures 4 and 5 respectively. From these figures, it reveals that the solution is unique when $S = S_c$, while dual solution exists up to $S_c < S < 1$ and no solutions for $S < S_c$. One way further note that as the ferromagnetic parameter increases, both the skin friction coefficient and the heat transfer rate at the wall surface decrease.

Figures 6 and 7 depict the variation of the skin friction coefficient $f''(0)$ and heat transfer rate $\theta'(0)$ with the stretching/shrinking parameter λ, for different values of nonlinear stretching parameter n. We also note that dual solution exists for a specific range of values of the nonlinear stretching parameter. The aforesaid observations may be summarized as follows:

(i) For $\lambda_c < \lambda < 0$, dual solutions exist.

(ii) When $\lambda = \lambda_c$, the solution exists and is unique.

(iii) For $\lambda < \lambda_c$, no solution exists.

(iv) With an increase in n, there is a reduction in the skin friction coefficient and the heat transfer rate.

(v) As the nonlinear stretching parameter n increases, the range of similarity solution and that of the existence of dual solutions are both enlarged.

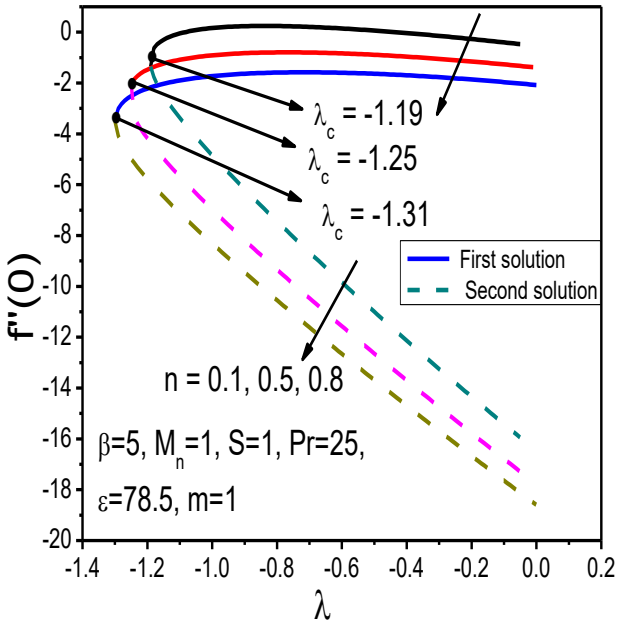

Figure 6. Change in skin friction coefficient for different values of n and λ_c .

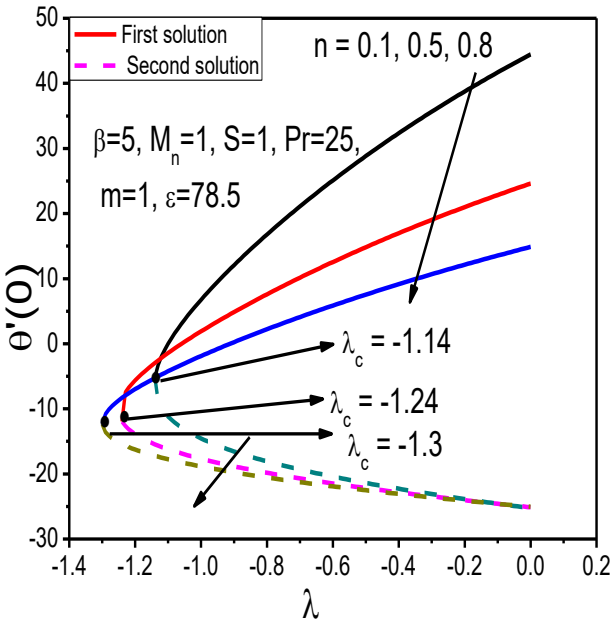

Figure 7. Change in heat transfer rate for different values of n and λ_c .

The effects of ferromagnetic parameter β on velocity and temperature distribution are shown in figures 8 and 9. These figures reveal that although the biomagnetic fluid velocity is enhanced as the ferromagnetic parameter increases for both cases (first and second solution), the fluid temperature is diminished, as the value of β rises. Here β is a ferromagnetic parameter and increment of the ferromagnetic parameter results in increment of the magnetic force. For this formulation this results to the increment of the resistance to the flow which is detected as velocity decrement and temperature increment. This signifies that the momentum boundary layer thickness becomes thinner with a rise in the value of the parameter β. For temperature distribution, since induce magnetic interaction parameter slow down the flow motion while passing the sheet which gives more time to the heat dissipates to the flow. This causes enhancement the temperature and simultaneously the thermal boundary layer thickness also gets thicker.

Figures 10 and 11 show that the effect of nonlinear stretching parameter (n) on the velocity and temperature distributions for a particular situation, when $\beta = 10,\ S = 1,\ M_n = 1,\ \lambda = 1,\ m = 1$. Figure 10 indicates that the velocity of the biomagnetic fluid is significantly reduced throughout the flow field as n is increased, in the case of the first solution. This signifies that the momentum boundary layer thickness becomes thinner with a rise in the value of the parameter n. But the result is to the contrary in the case of the second solution, except at points very close to the sheet. Figure 11 shows

that temperature reduces with increase in n, in the case of the first solution, while for the second solution, a reverse trend is observed.

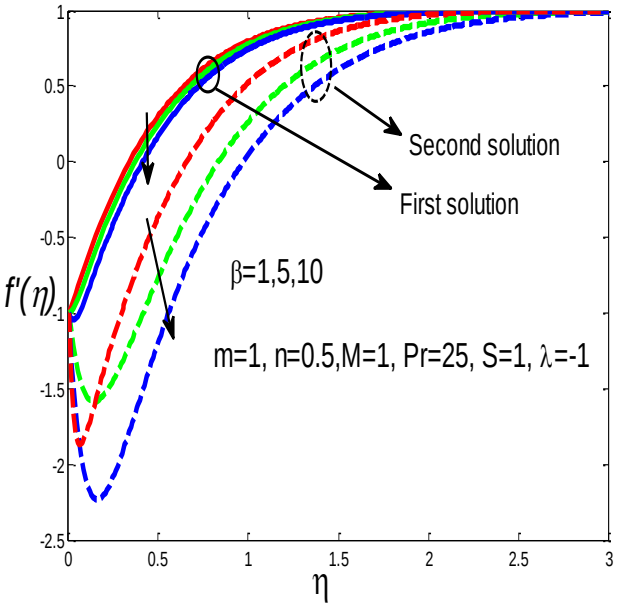

Figure 8. Velocity profiles, $f'(\eta)$ for different values of β.

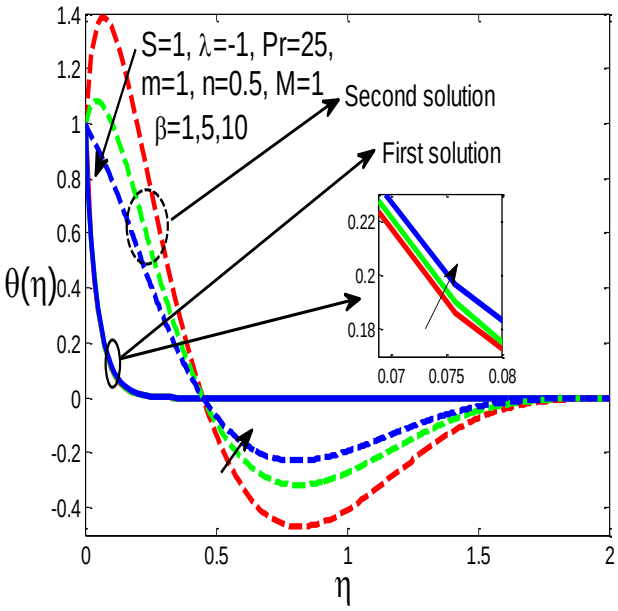

Figure 9. Temperature profiles, $\theta(\eta)$ for different values of β.

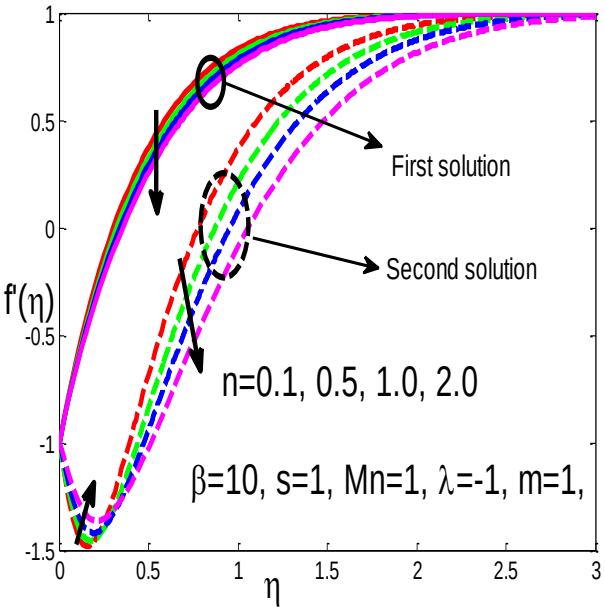

Figure 10. Velocity profiles, $f'(\eta)$ for different values of n.

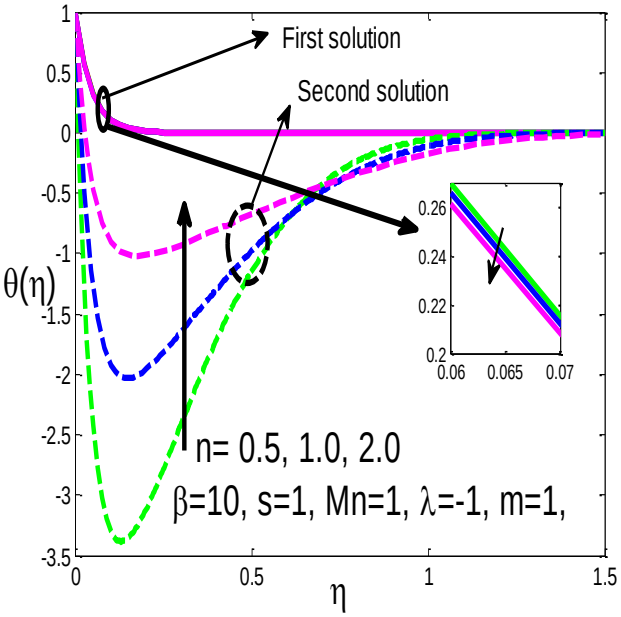

Figure 11. Temperature profiles, $\theta(\eta)$ for different values of n.

The effect of suction parameter S on velocity and temperature distributions can be found from figures 12 and 13. According to the first solution (cf. Figure 12), the fluid velocity increases, as the suction velocity enhances, while a reverse trend is observed in the case of the second solution. This can be interpreted physically by saying that since during suction, the fluid in the vicinity of the wall is sucked away, the boundary layer thickness is reduced due to suction and thereby the fluid velocity is enhanced. Figure 13 demonstrates that the fluid temperature is reduced as the quantum of suction increases. This implies that the thermal boundary layer thickness decreases with as suction proceeds. This causes an increase in the rate of heat transfer. However, this is the observation from the first solution. A reverse trend is found to occur, if we consider the second solution. This observation implies that as the fluid is brought closer to the surface, the thermal boundary layer thickness diminishes.

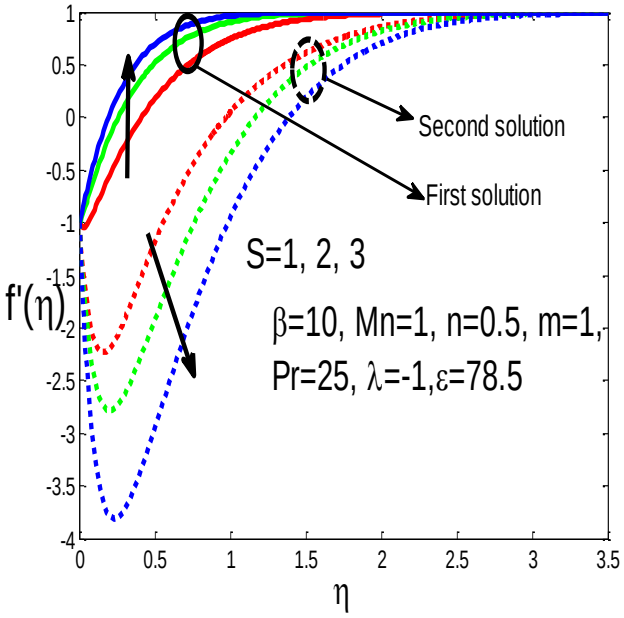

Figure 12. Velocity distribution for different values of S.

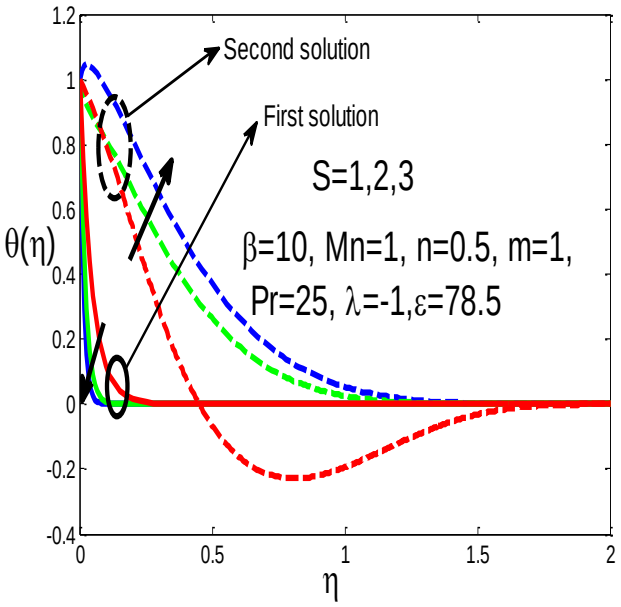

Figure 13. Temperature distributions for different values of S.

The impact of temperature exponent (m) on velocity and temperature distributions are displayed in figures 14 and 15, respectively. The dual velocity and temperature distributions are also presented in the same figures, alongside the first solutions. It may be noted that in the case of the first solution, as m increases the velocity decreases. But a reverse trend is observed in the case of the second solution. The results imply that increase in the fluid index is accompanied by a reduction in temperature boundary layer thickness also. These are the observations, when we consider the first solution. But for the second solution, the observations are a bit different. Also, the temperature exponent (m) parameter enhances the thermal overshoot near the sheet for the second solution.

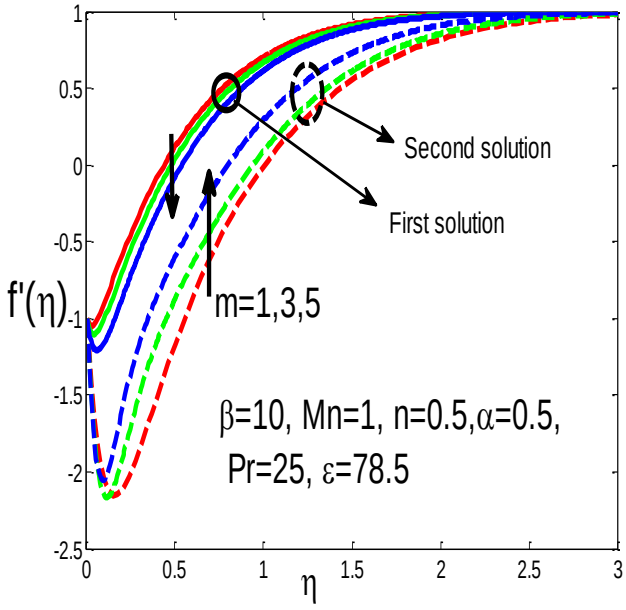

Figure 14. Velocity profiles, $f'(\eta)$ for different values of m.

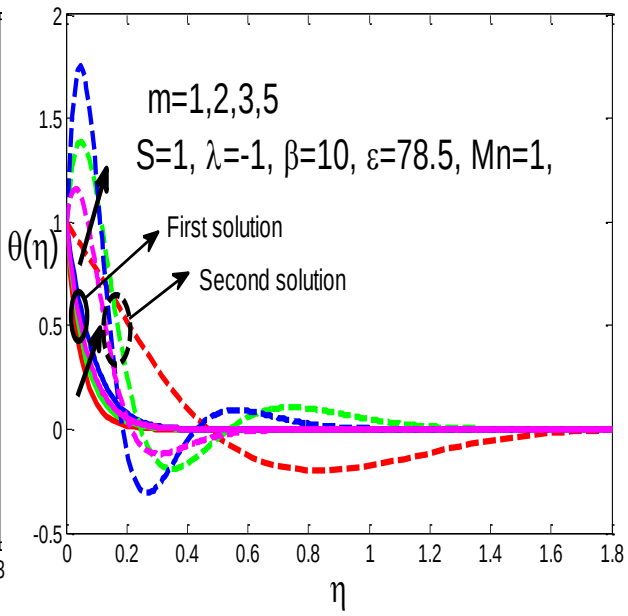

Figure 15. Temperature profiles, $\theta(\eta)$ for different values of m.

4. Concluding remarks

The paper is devoted to a theoretical study on the flow of a biomagnetic fluid, by using Lie group transformation method over a stretching/shrinking sheet, under the influence of a magnetic field generated owing to the presence of a magnetic dipole. The governing partial differential equations are transformed into nonlinear ordinary differential equations and solved numerically using BVP4C Matlab package. The effects of dimensionless governing parameters on velocity and temperature profiles of the flow are discussed with the help of graphs. Numerical computations are carried out and discussed for skin friction coefficient and local Nusselt number. Based on the present study we can make the following concluding remarks:

(i) The dual solutions exist only in the case of a shrinking sheet.

(ii) The stability analysis emphasizes the existence of dual solutions, out of which only one is stable and can be realized physically. But the second solution is not so.

(iii) With increase in the ferromagnetic effect during the fluid flow, the velocity, temperature and thermal boundary layer thickness are reduced.

(iv) The ferromagnetic parameter acts as the controlling parameter and it bears the potential to increase/reduce the thickness of the boundary layer.

(v) With rise in suction rate/ skin friction the fluid temperature increases.

(vi) With increase in nonlinear stretching, both the heat transfer rate and skin friction are reduced.

(vii) In fine, we would like to make a mention that both the physical parameters S and Re of the problem depend on "x", which plays the role of a scaling parameter. The present solution is comparable with those reported in [42] and [43]. In the solution we obtain, "x" is considered to be small and the magnetic field gradients are derived from the power series expansion in powers of x (cf. Anderson and Valnes [46]; Tzirtzilakis and Tanoudis [7]).

Thus although the general problem is non-similar, the solution presented here is valid only for small values of x.

(viii) As an important scope for future work, one can try the general problem, where x is not restricted to only small values of x. However, the present work will have its importance in validating the results of a non-similar problem.

Authors' contributions

M. Ferdows designed the study, developed the main conceptual ideas and were in charge of overall direction and planning. **G. Murtaza** developed the theoretical framework, performed the analytical calculations, Lie group transformation and performed the numerical simulations. **J. C. Misra** played an important role in making the proper presentation of the manuscript and also in discussing and interpreting the results. **Tzirtzilakis and Alsenafi** were interpreting the results and discussion, **G. Murtaza** and **M. Ferdows** helped to draft the manuscript. All authors discussed the results and commented on the manuscript and approved the final version of this manuscript.

Conflict of interest

The authors declare that they have no conflict of interest.

References

1. J. C. Misra, A. Sinha, G. C. Shit, Flow of a biomagnetic viscoelastic fluid: application to estimate of blood flow in arteries during electromagnetic hyperthermia, a therapeutic procedure for cancer treatment, *App. Math. Mech. Engl.,* **31** (2010)**,** 1405–1420.
2. P. W. Nelson, M. A. Gilchrist, D. Coombs, J. M. Hyman, A. S. Perelson, An age-structured model of HIV infection that allow for variations in the production rate of viral particles and the death rate of productively infected cells, *Math. Biosci. Eng*., **1** (2004), 267–288.
3. J. Wang, X. Dong, Analysis of an HIV infection model incorporating latency age and infection age, *Math. Biosci. Eng*., **15** (2018), 569–594.
4. Y. Haik, C. J. Chen, V. Pai, Development of biomagnetic fluid dynamics. Proceedings of the IX international Symposium on Transport Properties in Thermal fluid engineering, *Singapore, Pacific center of thermal fluid engineering, June* 25–28: 121–126 (1996).
5. E. E. Tzirtzilakis, A Mathematical model for blood flow in magnetic field, *Phys. Fluids,* **17** (2005), 077103-1-14.
6. E. E. Tzirtzilakis, N. G. Kafoussias, Biomagnetic fluid flow over a stretching sheet with nonlinear temperature dependent magnetization, *Z. Angew. Math. Phys (ZAMP)*, **8** (2003), 54–65.
7. E. E. Tzirtzilakis, G. B. Tanoudis, Numerical study of biomagnetic fluid flow over a stretching sheet with heat transfer, *Int. J. Numer. Methods Heat Fluid Flow***, 13** (2003), 830–848.
8. G. M. Murtaza, E. E. Tzirtzilakis, M. Ferdows, Effect of electrical conductivity and magnetization on the biomagnetic fluid flow over a stretching sheet, *Z. Angew. Math. Phy. (ZAMP),* **68** (2017), 93.
9. M. Ferdows, G. M. Murtaza, E. E. Tzirtzilakis, F. Alzahrani, Numerical study of blood flow and heat transfer through stretching cylinder in presence of a magnetic dipole, *Z. Angew. Math. Mech.,* 2020, e201900278.
10. L. Zhang, M. B. Arain, M. M. Bhatti, A. Zeeshan, H. H. Sulami, Effects of magnetic Reynolds

number on swimming of gyrotactic microorganisms between rotating circular plates filled with nanofluids, *Appl. Math. Mech. Engl. Ed.*, **41** (2020), 637–654.
11. M. M. Bhatti, M. Marin, A. Zeeshan, R. Ellahi, S. I. Abdelsalam, Swimming of motile gyrotactic microorganisms and nanoparticles in blood flow through Anisotropically tapered arteries, *Front. Phys.*, **8** (2020), 95.
12. M. M. Bhatti, A. Zeeshan, R. Ellahi, Heat transfer analysis on peristaltically induced motion of particle-fluid suspension with variable viscosity: clot blood model, *Comput. Meth. Prog. Bio.*, **137** (2016), 115–124.
13. M. M. Bhatti, A. Zeeshan, R. Ellahi, Endoscope analysis on peristaltic blood flow of Sisko fluid with Titanium magneto-nanoparticles, *Comput. Biol. Med*., **78** (2016), 29–41.
14. S. Mukhopadhyay, Heat transfer in a moving fluid over a moving non-isothermal flat surface, *Chin. Phys. Lett.*, **28** (2011), 124706.
15. K. Vajravelu, G. Sarojamma, K. Sreelakshmi, C. H. Kalyani, Dual solutions of an unsteady flow, heat and mass transfer of an electrically conducting fluid over a shrinking sheet in the presence of radiation and viscous dissipation, *Int. J. Mechan. Sci.*, **130** (2017), 119–132.
16. P. M. Krishna, N. Sandeep, R. Reddy, V. Sugunamma, Dual solutions for unsteady flow of powell-Eyring fluid past an inclined stretching sheet, *J. Naval Archit. Mar. Eng.*, **13** (2016)**,** 89–99.
17. K. Naganthran, R. Nazar, Dual solutions of MHD stagnation-point flow and heat transfer past a stretching/shrinking sheet in a porous medium, *4th International Conference on Mathematical Science AIP Conf.*, **1830** (2017), 020038-1-020038-8.
18. E. H. Hafidzuddin, R. Nazar, N. M. Arifin, I. Pop, Boundary layer flow and heat transfer over s permeable exponentially stretching/shrinking sheet with generalized slip velocity, *J. Appl. Fluid Mechan.*, **9** (2016)**,** 2025–2036.
19. T. R, Mahapatra, S. K. Nandy, I. Pop, Dual solutions in magnetohydrodynamics stagnation point flow and heat transfer over a shrinking surface with partial slip, *J. Heat Transfer, ASME,* **136** (2014)**,** 104501: 1–6.
20. R. Dhanai, P. Ranaa, L. Kumar, Multiple solutions in MHD flow and heat transfer of Sisko fluid containing nanoparticles migration with a convective boundary condition: Critical points, *Eur. Phys. J. Plus,* **131** (2016), 142.
21. M. H. M. Yasin, A. Ishak, I. Pop, MHD heat and mass transfer flow over a permeable stretching/shrinking sheet with radiation effect, *J. Magnet. Magnet. Mater.*, **407** (2016), 235–240.
22. I. S. Awaludin, P. D. Weidman, A. Ishak, Stability analysis of stagnation-point flow over a stretching/shrinking sheet, *AIP Advances,* **6** (2016), 0453081-7.
23. U. Mishra, G. Singh, Dual solutions of mixed convection flow with momentum and thermal slip flow over a permeable shrinking cylinder, *Comput. Fluids*, **93** (2014), 107–115.
24. M. Pakdemirli, M. Yurusoy, Similarity transformations for partial differential equations, *Soc. Ind. Appl. Math.,* 4**0** (1998), 96–101.
25. G. W. Bluman, S. Kumei, *Symmetries and differential equations,* Applied mathematical sciences, *Newyork: Springer-Verlag*; 1991.
26. K. S. Prabhu, R. Kandasamy, R. Saravanan, Lie group analysis for the effect of viscosity and thermophoresis particle deposition on free convective heat and mass transfer in the presence of suction/injection, *Theor. Appl. Mech.,* (2009), 275–298.

27. M. Jalil, S. Asghar, M. Mushtaq, Lie group analysis of mixed convection flow with mass transfer over a stretching surface with suction or injection, *Math. Probl. Eng.*, **2010** (2010), 1–14.
28. M. G. Reddy, Lie group analysis of heat and mass transfer effects on steady MHD free convection dissipative fluid flow past an inclined porous surface with heat generation, *Theoret. Appl. Mech.*, **39** (2012), 233–254.
29. M. M. Rashidi, E. Momoniat, M. Ferdows, A. Basiriparsa, Lie group solution for free convective flow of a nanofluid past a chemically reacting horizontal plate in a porous media, *Math. Probl. Eng.*, **2014** (2014), 1–21.
30. M. Ferdows, M. J. Uddin, A. A. Afify, Scaling group transformation for MHD boundary layer free convective heat and mass transfer flow past a convectively heated nonlinear radiating stretching sheet, *Int. J. Heat Mass Transfer,* **56** (2013),181–187.
31. J. C. Misra, A. Sinha, Effect of thermal radiation on MHD flow of blood and heat transfer in a permeable capillary in stretching motion, *Heat Mass Transfer*, **49** (2013), 617–628.
32. A. Sinha, J. C. Misra, Effect of induced magnetic field on magnetohydrodynamic stagnation point flow and heat transfer on a stretching sheet, *J. Heat Transfer, ASME*, **136** (2014), 112701:1–11.
33. J. C. Misra, S. Chandra, Electroosmotically actuated oscillatory flow of a physiological fluid on a porous micro-channel subjected to an AC electric field having dissimilar frequencies, *Cent. Euro. J. Phys.*, **12** (2013), 274–285.
34. J. C. Misra, S. Chandra, H. Herwig, Flow of a micro polar fluid in a micro-channel under the action of an alternating electric field: Estimates of flow in bio-fluidic devices, *J. Hydrodyn.*, **27** (2015), 350–358.
35. J. C. Misra, S. D. Adhikary, MHD oscillatory channel flow, heat and mass transfer of a physiological fluid in presence of chemical reaction, *Alex. Engng. J.*, **55** (2016), 287–297.
36. J. C. Misra, S. D. Adhikary, Flow of a Bingham fluid in a porous bed under the action of a magnetic field, *Eng. Sci. Technol.*, **20** (2017), 973–981.
37. M. Hatami, J. Hatami, D. D. Ganji, Computer simulation of MHD blood conveying gold nanoparticles as a third grade non-Newtonian nanofluid in a hollow porous vessel, *Comput. Method. Program. Biomed.*, **113** (2014), 632–641.
38. D. S. Chauhan, R. Agrawal, MHD flow through a porous medium adjacent to a stretching sheet: Numerical and an approximate solution, *Eur. Phys. J. Plus*, **126** (2011), 47.
39. M. W. A. Khan, M. I. Khan, T. Hayat, A. Alsaedi, Numerical solution of MHD flow of power law fluid subject to convective boundary conditions and entropy generation, *Comput. Method. Program. Biomed.*, **188** (2019), 105262.
40. U. S. Mahabaleshwar, K. R. Nagaraju, P. N. V. kumar, M. N. Nadagoud, R. Bennacer, D. Baleanu, An MHD viscous liquid stagnation point flow and heat transfer with thermal radiation and transpiration, *Therm. Sci. Eng. Progress*, **16** (2020), 100379.
41. U. S. Mahabaleshwar, K. R. Nagaraju, P. N. V. Kumar, M. N. Nadagouda, R. Bennacer, M. A. Sheremet, Effects of Dufour and Soret mechanisms on MHD mixed convective-radiative non-Newtonian liquid flow and heat transfer over a porous sheet, *Therm. Sci. Eng. Progress*, **16** (2020), 100459.
42. K. Nagranthran, R. Nazar, I. Pop, Unsteady stagnation point flow and heat transfer of a special third grade fluid past a permeable stretching/shrinking sheet, *Sci. Rep.*, **6**(2016), 24632.
43. K. Bhattacharyya, Dual solutions in unsteady stagnation-point flow over a shrinking sheet, *Chin.*

Phys. Lett., **28** (2011), 084702.
44. H. S. Hassan, Symmetry analysis for MHD viscous flow and heat transfer over a stretching sheet, *Appl. Math.*, **6(1)** (2015), 78–94.
45. S. D. Harris, D. B. Ingham, I. Pop, Mixed convection Boundary-layer flow near the stagnation point on a vertical surface in a porous medium: Brinkman model with slip, *Transp. Porous Media*, **77** (2009), 267–285.
46. H. I. Andersson, O. A. Valnes, Flow of a heated ferrofluid over a stretching sheet in the presence of a magnetic dipole, *Acta Mechan.*, **128** (1998), 39–47.

AIMS Press